Conceptual development of a novel photovoltaic-thermoelectric system and preliminary economic analysis

Guiqiang Li[a, *]

ligq@mail.ustc.edu.cn

Xudong Zhao[b, *]

Xudong.zhao@hull.ac.uk

Jie Ji[a]

[a]Department of Thermal Science and Energy Engineering, University of Science and Technology of China, 96 Jinzhai Road, Hefei City 230026, China

[b]School of Engineering, University of Hull, Hull HU6 7RX, UK

*Corresponding authors.

Abstract

Photovoltaic-thermoelectric (PV-TE) hybrid system is one typical electrical production based on the solar wide-band spectral absorption. However the PV-TE system appears to be economically unfeasible owing to the significantly higher cost and lower power output. In order to overcome this disadvantage, a novel PV-TE system based on the flat plate micro-channel heat pipe was proposed in this paper. The mathematic model was built and the performance under different ambient conditions was analyzed. In addition, the annual performance and the preliminary economic analysis of the new PV-TE system was also made to compare to the conventional PV system. The results showed that the new PV-TE has a higher electrical output and economic performance.

Keywords: Photovoltaic-thermoelectric; Micro-channel heat pipe; Mathematic model; Economic analysis

Nomenclature

A

area of PV

a_{teg}

cross-sectional area of a P or N leg, m^2

C_{fx}

local friction coefficient

C_p

specific heat of air, kJ/(kg K)

E_{con}

heat flux via conduction, W

E_{cov}

heat flux via convection, W

E_{in}

solar energy absorbed by selective absorbing coating, W

E_{pv}

PV electrical output, W

E_{rad}

heat flux via radiation, W

G

solar radiation, W m^{-2}

h_{cov}

coefficient of convection heat transfer, W/(m^2 K)

h_{rad}

coefficient of radiation heat transfer, W/(m^2 K)

I

electrical current, A

K

thermal conductivity of heat pipe, W m^{-1} K^{-1}

k_{air}

thermal conductivity of air, W m^{-1} K^{-1}

k_{teg}

thermal conductivity of TEG, W m^{-1} K^{-1}

L

length of the heat sink, m

L_{hp}

length of heat pipe, m

l_{teg}

height of TEG, m

n_{teg}

numbers of PN junction

Nu

Nuselt number

Pr

Prandtl number

Q_{tegh}

energy that passed in hot side of the TEG, W

Q_{tegl}

energy that passed out of cold side of the TEG, W

R_{conf}

resistance of the heat conduction in heat sink, K W^{-1}

R_{covf}

thermal resistance of convection Heat transfer between heat sink and ambient air, K W^{-1}

R_{ct1}

thermal contact resistance between selective absorbing coating and heat pipe, K W^{-1}

R_{ct2}

thermal contact resistance between heat pipe and the TEG, K W^{-1}

R_{ct3}

thermal contact resistance between TEG and heat sink, K W^{-1}

R_{fin}

thermal resistance of the heat sink, K W^{-1}

r_{teg}

electrical resistivity of P or N junction, Ω m

Re

Reynolds number

St

Stanton number

S_1

cross section area of the heat sink, m^2

S_2

total area of the heat sink, m^2

T_a

temperature of ambient air, K

T_h

temperature of the evaporating side of the heat pipe, K

T_{tegh}

the temperature of hot side of TEG, K

T_{tegl}

temperature of the cold side of TEG, K

T_l

temperature of the condensate side of the heat pipe, K

T_p

temperature of absorbing coating, K

T_{sky}

temperature of sky, K

u

wind speed, m/s

Greek letters

α

heat diffusivity, m^2/s

α_b

absorptivity of absorbing coating

α_{teg}

Seebeck coefficient, $V\ K^{-1}$

δ

Stefan-Boltzmann constant, $W\ m^{-2}\ K^{-4}$

ε

reflectivity of absorbing coating

μ

viscosity (dynamic)[2], $N\ s/m^2$

ν

kinematic viscosity, m^2/s

ρ

density of air, kg/m^3

1 Introduction

Solar power generation is one of the important applications for solar energy, and the low cost and high efficiency solar power generation has always been the focus of the solar energy basic research. Currently, Photovoltaic (PV) is the most common and commercialized way for solar electrical generation. Nevertheless, the conventional materials can convert effectively only photons of energy close to the semiconductor band gap [1]. For example, the single junction Si technologies are limited to maximum efficiencies in the order of 30% [2], which leads to most of the absorbed energy is converted into the thermal energy, increasing the PV temperature and leading to further efficiency reduction [3–5]. Thus the way to utilize the thermal energy to produce the electricity is important for fully exploiting the wide solar spectrum.

Thermoelectric generation (TEG) is a device to utilize the Seebeck effect to convert heat from solar energy directly into electrical energy through the movement of charge carriers induced by a temperature span across it [6]. Compared to conventional electrical power generator systems, the TEG theoretically can own many advantages such as being simple and highly reliable, having no moving parts, and being environmentally friendly. From the view of the fully solar spectrum application and the installment convenience, it would be suitable for combination the PV and TE.

Many researchers paid more attentions on the combination of the thermoelectric and the photovoltaic technology in a hybrid system in recent years [7–10]. There are main two types: splitting system and integrating system. Kraemer et al. proposed a general optimization methodology of solar spectrum splitting for PV-TE system [11]. Mizoshiri et al. used thin-film thermoelectric modules to combine with photovoltaic [12]. Fleurial indicated that the PV-TE may be integrated with the solar concentrator, which can obtain a high electrical output [13]. Van Sark predicted the feasibility of the splitting PV–TEG that the efficiency can be enhanced up to 23%, however the heat losses has been neglected in the simulation [14]. Hashim et al. built the model for geometry optimization of thermoelectric devices in a hybrid PV-TE system [15]. Bjørk and Nielsen analyzed the performance of a combined solar photovoltaic (PV) and thermoelectric generator (TEG) device [16]. Lin et al. coupled the temperatures and power outputs in hybrid photovoltaic and thermoelectric modules [17]. Da et al. studied the light trapping to solar energy utilization for a novel photovoltaic–thermoelectric hybrid system to fully utilize solar spectrum [18]. Cui et al. designed a novel concentrating photovoltaic–thermoelectric system incorporated with phase change materials [19]. Wang et al. took the experiment on the high-performance photovoltaic–thermoelectric hybrid device using the dye-sensitised solar cell [20].

However, whatever the splitting system or integrating system, the pair-arrangement between the PV and TE modules appears to be economically unfeasible, owing to the significantly higher cost and lower power output of the TE module relative to the PV module.

Heat pipes are efficient heat transfer devices that utilize latent heat of vaporization to transport heat over a long distance with small temperature gradient [21]. Micro-channel heat pipe (MCHP) has a higher heat transfer and smaller temperature gradient performance due to the micro-channel structure [22]. Li et al. made the experiment and simulation on the solar thermoelectric generator using the micro-channel heat pipe array, and the system saved a mass of TEG modules and reduced lots of the cost which showed the significant advantage than the TE without the heat pipe in series [23]. In addition, the non-uniform temperature can seriously affect the efficiency of the PV and TEG [24,25]. Thus, combing the flat plate micro-channel heat pipe and PV and TE, can homogenize the heat flux distribution for the high electrical output. At the same time, the flat plate micro-channel heat pipe can be attached to PV and TE closely, which can further reduce the contact thermal resistance between them.

Therefore, in this paper the conceptual of a novel photovoltaic-thermoelectric system was developed, which included the PV, the micro-channel heat pipe, the TE and the heat sink. The different ambient parameters were all considered to analyze the system performance. Furthermore, the conventional PV system was introduced to compare to the new PV-TE system. In addition, the preliminary economic analysis was carried out based on the whole year performance evaluation.

2 System description

The novel photovoltaic-thermoelectric system was shown in Fig. 1. The PV modules were attached to the upper surface of the evaporator of the MCHP while the TE modules were attached to the lower surface of the condenser. During operation, the solar energy imposed on PV modules on the upper surface of the MCHP's evaporator, then the thermal energy was conveyed to MCHP's condenser, by means of the evaporation of the working fluid within the MCHP. In the condenser, the heat was released via condensation of the MCHP working fluid and was then transferred to the attached TE modules. This created a temperature gradient

across the TE module, thus resulting in a thermal to electrical conversion by means of the‘Peltier effect’. The cooling structure of TEG was air cooling, whose performance was decided by the cooling structure, the ambient temperature and the wind speed.

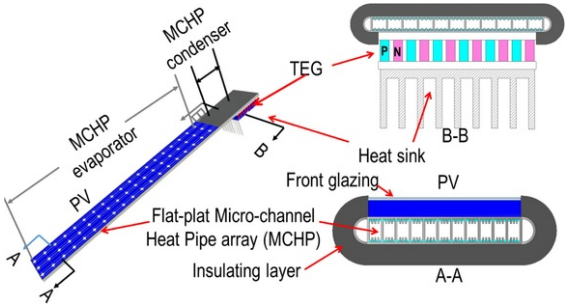

Fig. 1 Schematic diagram of the novel photovoltaic-thermoelectric system.

3 Mathematic model

The heat transfer process of the new PV-TE system was shown in Fig. 2. According to heat balance, the energy conducted by the heat pipe can be expressed as below,

$$E_{in} = E_{pv} + E_{con} + E_{rad} + E_{cov} \quad (1)$$

where E_{in} is the solar energy absorbed by the PV-TE system. It can be expressed as below,

$$E_{in} = (\tau\alpha)_{pv} AG \quad (2)$$

where $(\tau\alpha)_{pv}$ and A are the effective transmittance-absorption product of the PV and PV area respectively. G is the solar radiation.

$$(\tau\alpha)_{pv} = \frac{\tau_\alpha \tau_\rho \alpha}{1-(1-\alpha)\rho_g} \quad (3)$$

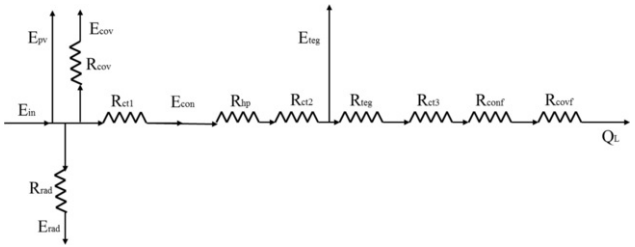

Fig. 2 Schematic of the heat transfer network of the new PV-TE system.

The electrical output is given by:

$$E_{pv} = (\tau\alpha)_{pv} AG\eta_r[1-\beta_{pv}(T_p - T_r)] \quad (4)$$

where T_p is the PV temperature. β_{pv} is the temperature coefficient of PV efficiency. T_r is the reference temperature.

The electrical efficiency of the PV can be expressed as:

$$\eta_{sys-pv} = \frac{E_{pv}}{AG} \quad (5)$$

E_{rad} is the energy transferred to the space via the radiation, which is expressed as below,

$$E_{rad} = h_{rad} A(T_p - T_{sky}) \quad (6)$$

h_{rad} can be defined as

$$h_{rad} = \varepsilon\delta\left(T_{sky}^2 + T_p^2\right)(T_{sky} + T_p) \quad (7)$$

T_{sky} can be defined as

$$T_{sky} = 0.0552T_a^{1.5} \quad (8)$$

where T_p is temperature of the PV and T_a is the temperature of ambient air.

E_{cov} is the energy convection between the PV and the ambient air, which is expressed as

$$E_{cov} = h_{cov}A(T_p - T_a) \quad (9)$$

where h_{cov} can be defined as

$$h_{cov} = 6.5 + 3.3u \quad (10)$$

The energy conducted via the heat pipe can also be expressed in several ways. The heat flux pass through the thermal contact resistance between the PV and heat pipe can be expressed as,

$$E_{con} = (T_p - T_h)/R_{ct1} \quad (11)$$

where T_h is the temperature of the evaporating side of the heat pipe.

The heat flux conducted by the heat pipe can be expressed as,

$$E_{con} = KL_{hp}(T_h - T_l) \quad (12)$$

where K is the thermal conductivity of the heat pipe, L_{hp} is the length of the heat pipe and T_l is the temperature of the condensate side of the heat pipe.

The heat flux pass through the thermal contact resistance between heat pipe and the TEG (R_{ct2}) can be defined as,

$$E_{con} = (T_l - T_{tegh})/R_{ct2} \quad (13)$$

where T_{tegh} is the temperature of the hot side of the TEG.

The energy that passed through the hot side of the TEG can be defined by following equation.

$$Q_{tegh} = 2n_{teg}\alpha_{teg}T_{tegh}I + 2n_{teg}\frac{a_{teg}k_{teg}}{l_{teg}}\Delta T - \frac{1}{2}I^2 2n_{teg}\frac{r_{teg}l_{teg}}{a_{teg}} \quad (14)$$

Similarly, the heat through the cold side of TEG can be expressed as

$$Q_{tegl} = 2n_{teg}\alpha_{teg}T_{tegl}I + 2n_{teg}\frac{a_{teg}k_{teg}}{l_{teg}}\Delta T + \frac{1}{2}I^2 2n_{teg}\frac{r_{teg}l_{teg}}{a_{teg}} \quad (15)$$

where Q_{tegh} is the energy that passed in hot side of the TEG, Q_{tegl} is the energy that passed in cold side of the TEG, n_{teg} is the numbers of PN junction, α_{teg} is the Seebeck coefficient, I is the current, K_{teg} is thermal conductivity of TEG, l_{teg} is the length of TEG, T_{tegl} is the temperature of cold side of TEG, r_{teg} is the electrical resistivity of a P or N leg, a_{teg} is the Cross-sectional area of a P or N leg.

In a real system, TEG has to operate in the closed-circuit condition in order to deliver the power to external load. Under such circumstances, the heat flow through the TEG consists of both heat conduction and the Peltier heat. As a result, the ΔT can be replaced by Refs. [26–28].

$$\Delta T = (1 + ZT_M)(T_{tegh} - T_{tegl}) \quad (16)$$

where Z (= $\alpha_{teg}^2/\rho\cdot k$) is the thermoelectric figure of merit, T_M is givens as

$$T_M = \frac{(1+2s)T_{tegh} + T_{tegl}}{2(1+s)^2} \quad (17)$$

where s is the ratio of the load resistance to the internal resistance of the TE module. when s = 1, the electrical efficiency of the TEG can be expressed as:

$$\eta_{teg} = \frac{Q_{tegh} - Q_{tegl}}{Q_{tegh}} \tag{18}$$

The electrical efficiency of the system can be expresses

$$\eta_{sys-teg} = \frac{Q_{tegh} - Q_{tegl}}{AG} \tag{19}$$

This heat can also be expressed as the heat flux through the heat sink attached to the cold side of TEG.

$$Q_{tegl} = (T_{tegl} - T_a)/R_{fin} \tag{20}$$

where R_{fin} is the thermal resistance of the fin which clings to the cold side of TEG, and can be expressed as below,

$$R_{fin} = R_{conf} + R_{covf} + R_{ct3} \tag{21}$$

where R_{conf} is the resistance of the heat conduction of the heat sink and R_{ct3} is the thermal contact resistance between the TEG and the heat sink.

$$R_{conf} = \frac{H}{K_{fin} S_1} \tag{22}$$

where H is the height of the heat sink, K_{fin} is the thermal conductivity of the fin and S_1 is the cross section area of the heat sink.

In order to attain the value of R_{covf} which is the thermal resistance of convection heat transfer between fin and ambient air, the convection heat transfer coefficient h_{covf} can be obtained [29].

$$C_{fx} = 0.0592\, Re_x^{-1/5} \tag{23}$$

$$Re_x = \frac{\rho u x}{\mu} \tag{24}$$

where u, ρ, μ represent velocity, density and viscosity coefficient of the fluid respectively, x is the characteristic length of the fin. $\rho = 1.1614$ $\mathrm{kg\,m^{-3}}$, $\mu = 1.846 * 10^{-5}$ $\mathrm{N\,s\,m^{-2}}$.

$$Nu_x = \frac{h_x x}{k_{air}} = 0.332 Re_x^{\frac{1}{2}} \mathrm{Pr}^{\frac{1}{3}}, 0.6 \leqslant \mathrm{Pr} \leqslant 15 \tag{25}$$

$$\mathrm{Pr} = \frac{v}{\alpha} = \frac{\mu C_p}{k_{air}} \tag{26}$$

where v is the kinematic viscosity, h_x is the local heat transfer coefficient along the length of the fin, k_{air} is the thermal conductivity of air, C_p is the specific heat capacity of air, α is the heat diffusivity. $v = 1.589 * 10^{-5}$ $\mathrm{m^2\,s^{-1}}$, $c_p = 1.007$ $\mathrm{kJ\,kg^{-1}\,K^{-1}}$, $\alpha = 2.25 * 10^{-5}$ $\mathrm{m^2/s}$.

Thus St_x can be obtained as below,

$$St_x = \frac{Nu_x}{Re_x \mathrm{Pr}} = \frac{h_x}{\rho C_p \mu_\infty} = 0.332 Re_x^{-1/2} \mathrm{Pr}^{-2/3} \tag{27}$$

$$St_x \mathrm{Pr}^{2/3} = C_{f,x}/2 \tag{28}$$

$$h_x = \frac{C_{f,x} \rho C_p u_\infty}{2\mathrm{Pr}^{2/3}} \tag{29}$$

And the local heat transfer coefficient h_x is obtained,

$$h_x = \frac{0.0296 x^{-1/5} \rho C_p \mu_\infty^{4/5}}{v^{-1/5} \cdot \mathrm{Pr}^{2/3}} \tag{30}$$

Therefore,

$$h_{covf} = \frac{1}{L} \int_0^L h_x dx \tag{31}$$

After finishing calculated tablet on the air, the average heat transfer coefficient can be expressed as:

$$h_{covf} = \frac{0.037 L^{-1/5} \rho C_p u_\infty^{4/5}}{\upsilon^{-1/5} \cdot \mathrm{Pr}^{2/3}} \tag{32}$$

Then the thermal resistance between the radiator and the air is:

$$R_{covf} = \frac{1}{h_{covf} S_2} = \frac{\upsilon^{-1/5} \cdot \mathrm{Pr}^{2/3}}{0.037 L^{-1/5} \rho C_p u_\infty^{4/5} S_2} \tag{33}$$

where S_2 is the total area of the fin.

Therefore the overall electrical efficiency of the PV-TEG system can be expressed as

$$\eta_{sys-pvte} = \eta_{sys-pv} + \eta_{sys-teg} \tag{34}$$

4 Performance analysis

The performance of the new PV-TE system was affected by the ambient parameters. In this section, different solar radiation, wind speed and ambient temperature were all considered to illustrate the PV-TE performance. In addition, the conventional PV system was also compared to this new system. The relative parameters are shown in Table 1. The relatively models and parameters values have been verified in [23,30,31].

Table 1 The relative parameters in the PV-TE system.

Parameter	Numerical
PV	
Area	$1.2 * 0.18$ m^2
Transmittance of front glazing on PV τ_α	0.09
Reflecance of front glazing on PV ρ_g	0.08
Absorptivity of PV α	0.9
PV efficiency η_r	14.2%
Thermal contact resistance between PV and heat pipe R_{ct1}	4×10^{-4} Ω
Thermal contact resistance between PV and the TEG R_{ct2}	1×10^{-4} Ω
Micro-channel heat pipe	
Thermal conductivity of heat pipe K	23,000 W/(m K)
Length of the heat pipe L_{hp}	1.25 m
Thermal contact resistance between TEG and heat sink R_{ct3}	1×10^{-4} Ω
TEG	
	241

Numbers of P or N junction n_{teg}	
Cross-section area of one P or N junction a_{teg}	1×10^{-8} m^2
Seebeck coefficient α_{teg}	1.35×10^{-4} V K^{-1}
Electrical resistivity of one P or N junction r_{teg}	3.35×10^{-8} Ω m
Height of TEG l_{teg}	3.4×10^{-3} m
Heat sink	
Height of the heat sink H	1×10^{-2} m
Length of the heat sink L	5×10^{-2} m
Cross section area of the heat sink S_1	1.2×10^{-4} m^2
Total area of the fins S_2	1.46×10^{-2} m^2

4.1 Different solar radiation

When the wind speed was 2 m/s and the ambient temperature was 298 K, the TEG hot and cold side temperature was shown in Fig. 3. With the solar radiation increase, the temperature difference of TEG showed a rise tendency.

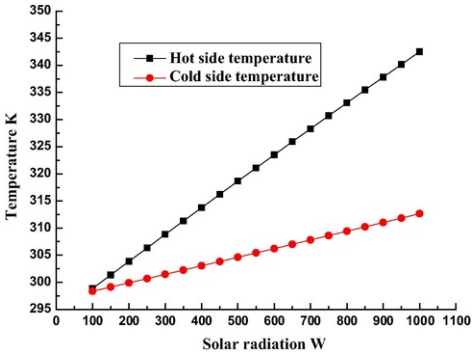

Fig. 3 TEG hot and cold side temperature at different solar radiation.

Corresponding to Fig. 3, when the solar radiation was low, the temperature difference of TEG was small, thus the electrical efficiency of TEG was close to the zero (Fig. 4). However, when the solar radiation was high, the electrical efficiency of TEG presented a trend of the rapid growth. On the other hand, with the hot side temperature increase, which means when the PV temperature increased, the PV electrical efficiency had a decrease tendency.

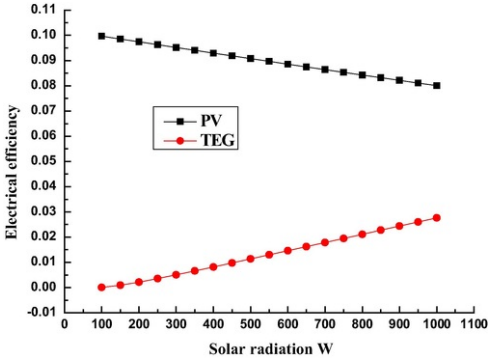

Fig. 4 Electrical efficiency of PV and TEG in PV-TE system at different solar radiation.

When the radiation was low, the electrical efficiency of TEG was small, so the system efficiency of TEG became lower. However, when the radiation was high, the electrical efficiency of TEG was larger, so the system efficiency of TEG became higher. Therefore with the solar radiation increased, the system efficiency of PV-TE presented the fall and then rise tendency (Fig. 5). For the conventional PV system, with the solar radiation increase, the PV temperature became higher, so the system efficiency presented a decrease tendency.

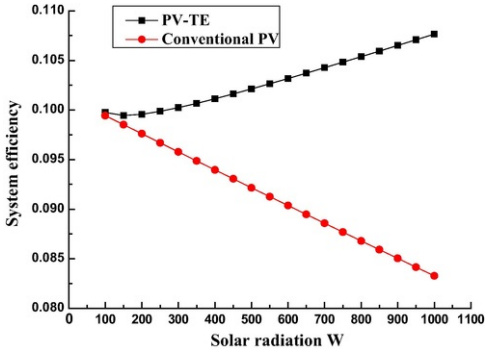

Fig. 5 System efficiency comparison between PV-TE and conventional PV at different solar radiation.

4.2 Different wind speeds

The wind speed increased will enhance the cooling of the heat sink, which would be benefit for the TEG. Nevertheless, the larger wind speed would also increase the thermal losses on the PV via the heat convection to the environment, which will decrease the hot side temperature of TEG and affect the TEG electrical efficiency negatively. Therefore, the comprehensive performance needed to evaluate on the specific working condition. Fig. 6 showed the variation curves of the hot and cold side temperature of TEG at different wind speeds when the solar radiation was 1000 W and the ambient temperature was 298 K. It is clearly that with the wind speed increase, the temperature difference of TEG became larger and then smaller. That also indicated that the TEG output would be higher then lower.

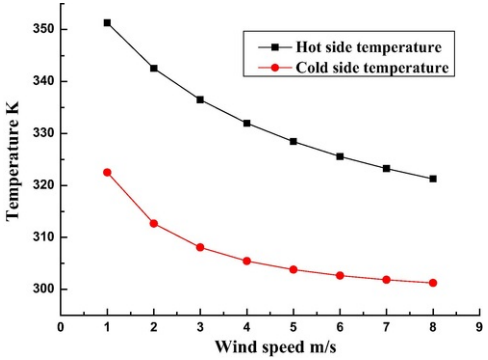

Fig. 6 TEG hot and cold side temperature at different wind speeds.

With the different wind speeds, the electrical efficiency of PV and TEG were shown in Fig. 7. The curve of the TEG electrical efficiency was in keeping with that of the temperature difference, which indicated a rise then fall tendency. For the PV efficiency, the curve presented a rising trend, but the rising amplitude became smaller, which means that when the wind speed increased to a high value, the PV electrical efficiency would be affected in a small range.

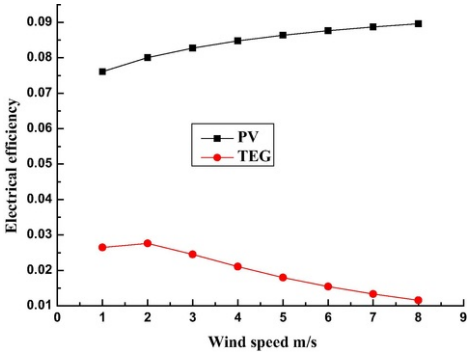

Fig. 7 Electrical efficiency of PV and TEG in PV-TE system at different wind speed.

The comparison between the PV-TE and conventional PV on the system efficiency was shown in Fig. 8. With the increase of the wind speed, the PV-TE system efficiency presented a rising than fall tendency. In the scope of the low wind speeds, the PV output increase was larger than the TEG output decrease. But in the scope of the high wind speed, the PV output increase was lower than the TEG output decrease, so the system efficiency decreased significantly.

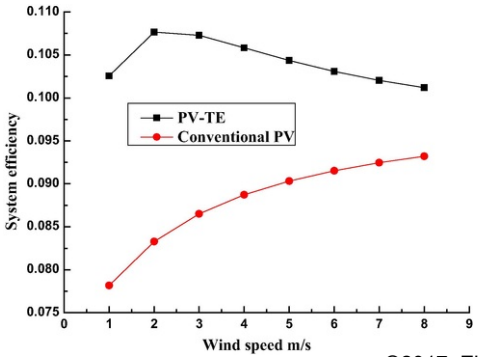

Fig. 8 System efficiency comparison between PV-TE and conventional PV at different wind speeds.

4.3 Different ambient temperature

When the solar radiation was 1000 W and the wind speed was 2 m/s, the hot and cold side temperature of TEG were all raised with the ambient temperature increase (Fig. 9). The temperature difference slightly became smaller when the ambient temperature became higher.

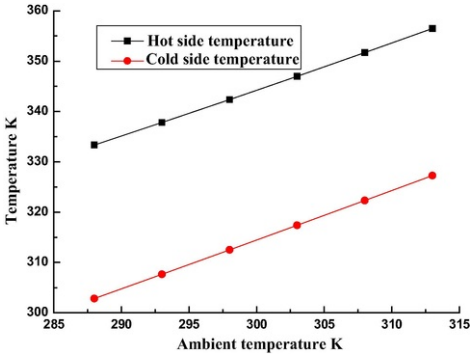

Fig. 9 TEG hot and cold side temperature at different ambient temperature.

In the PV-TE system, the TEG electrical efficiency changed in a small scope since the variation of the temperature difference of TEG was small (Fig. 10). But it is clearly that the PV electrical efficiency had a significant decrease tendency, because the PV temperature rose with the ambient temperature increase.

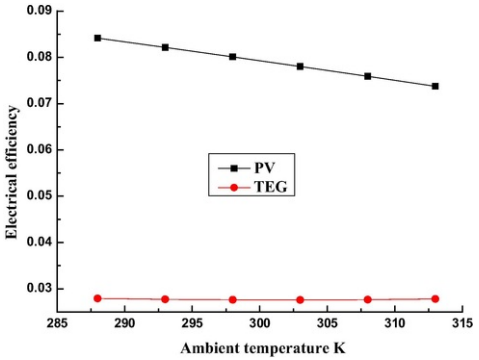

Fig. 10 Electrical efficiency of PV and TEG in PV-TE system at different ambient temperature.

The variation tendency of the PV-TE system and the conventional PV system were all downward with the increase of the ambient temperature, which was due to the higher temperature led to the lower PV efficiency. However, because of the TEG output, the new PV-TE system was still higher than the conventional PV system (see Fig. 11).

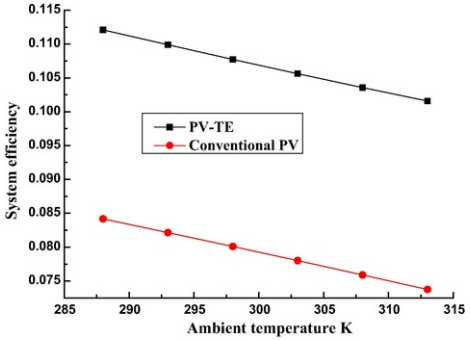

Fig. 11 System efficiency comparison between PV-TE and conventional PV at different ambient temperatures.

5 Annual output and preliminary economic analysis

To predict the annual performance of the new PV-TE system, a numerical simulation program written using Matlab has been developed. The Efficiency comparison of PV, novel PV-TE and conventional PV-TE with different solar radiations was shown in Fig. 12. The electrical efficiency of the conventional PV-TE is the highest one, and that of the PV is lowest one.

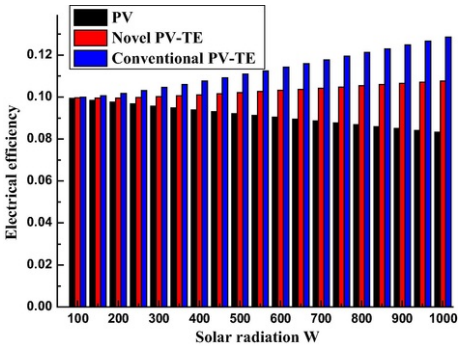

Fig. 12 Efficiency comparison of PV, novel PV-TE and conventional PV-TE.

Fig. 13 showed the flow chart of the computation process for the PV-TE system. In the present simulation, the PV-TE system would collect the solar energy. The weather data were provided by EnergyPlus. The weather data in half an hour is the average value, so the weather data changes every half an hour.

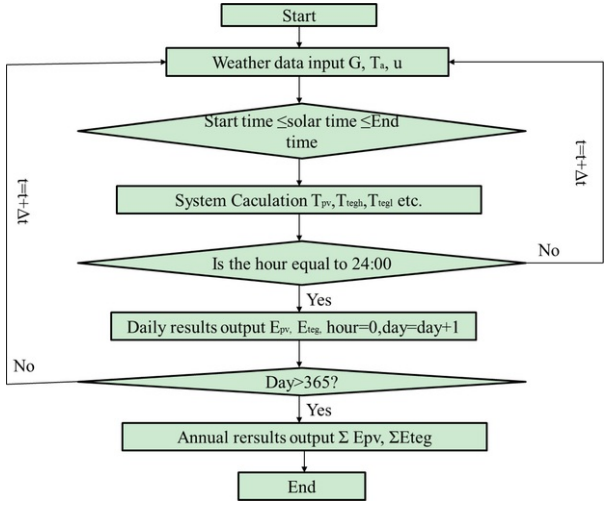

Fig. 13 Flow chart of the computation process for the PV-TE system.

For the conventional PV-TE system, the economic advantage to the conventional PV system is existent. So the key issue in this study is that whether the proposed new PV-TE has the advantages in the efficiency and the economy than the common PV system. The annual electricity outputs of the novel PV-TE system, the conventional PV-TE system and the PV system were shown in Fig. 14.

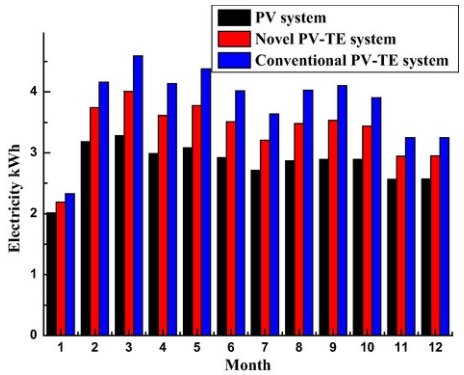

Fig. 14 Electricity production comparison of PV, novel PV-TE and conventional PV-TE systems in Hefei.

In winter, the electricity difference between the new PV-TE system and conventional PV system was lower than that in summer, which may be because the low ambient temperature was benefit for the conventional PV system. From Fig. 14, it can be seen that the new PV-TE system can attain more about 6.44 kW h annual electricity output than the conventional PV system with the same area in Hefei (31°53′N, 117°15′E) in the eastern region of China. And the conventional PV-TE system can attain more about 5.40 kW h annual electricity output than the novel PV-TE system.

From the view of the investment and return, the efficiency is just a factor, and the economic factors such as the ratio of output to input are also important. For the new PV-TE system, besides of the same PV area with the conventional PV, it has a micro-channel heat pipe, a TE module and a heat sink, and the extra costs were shown in Table 2. However, for the conventional PV-TE, due to the pair-arrangement between the PV and TE module, the extra costs is high with the same area, which can be approximately calculated ($¥22 * 1.2 * 0.18/0.055^2 = ¥1570$), which is about 41 times higher than the extra costs of the new PV-TE. At the same time, the extra annually electrical production of the conventional PV-TE is just 2 times higher ($(6.44 + 5.40)/6.44 \approx 2$) than that of the new PV-TE. Therefore, the new PV-TE has the economic advantage than the conventional PV-TE.

Table 2 Extra costs in novel PV-TE system.

Module	Micro-channel heat pipe	TEG	Heat sink
Cost	¥ 15.0	¥ 22.0	¥ 1.0

Therefore, in this section, the comparison between the new PV-TE system and the conventional PV system will be presented. The present section regards the economic analysis of the system, where the parameter concerning the electricity cost will be ¥1.20/kW h. The basic methodology is deployed for the calculation of the economic performance.

The coefficient that correlates a future cash flow with a present value is called the present value coefficient and is given by the following Eq. (35).

$$CF_{t=0} = \frac{CF_{t=0}}{(1+r)^n} \tag{35}$$

Where r is the interest rate.

The net present value (NPV), which is actually the present value of the total cash flows during the economic life cycle of a system, is given next by Eq. (36).

$$NPV = \sum_{j=1}^{n} \frac{B_{t=j} - C_{t=j}}{(1+r)^j} \tag{36}$$

where B is the present value of the benefit; C is the present value of the cost; j is the time period.

The Pay-Back-Period (PBP) is the time-period in years required for the NPV to reach a zero value and is found by solving Eq. (36) with NPV = 0. The higher NPV means the more profit during the life cycle. In this section, due to the two systems have the same area of PV, so it only needs to calculate the PBP of the extra investment. In this section, it is assumed that the labor and maintain costs of the new PV-TE system are the same as that of the conventional PV system. Thus the recovery cost of the extra investment will be achieve in six years (Fig. 15), which means from the sixth year, the new PV-TE system has a higher ratio of output to input than the conventional PV system. Therefore, the new PV-TE system constitutes from the techno-economic aspect a more efficient solution for the power production.

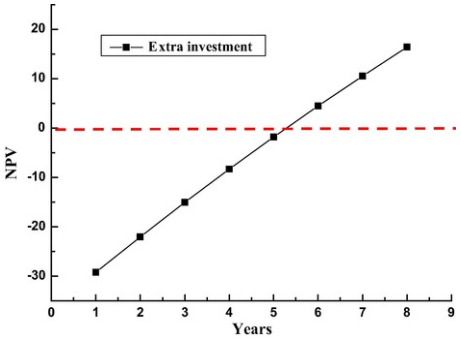

Fig. 15 Pay-Back-Period of the novel PV-TE system.

6 Conclusion

In this paper, the conceptual development of a novel photovoltaic-thermoelectric system was presented. The performance comparison between the new PV-TE system and the conventional PV system was demonstrated under different ambient conditions. The preliminary economic analysis was also made based on NPV, which indicated that the PBP of the additional investment is approximately six years.

In conclusion, the new PV-TE system has many advantages than the conventional PV-TE system and PV system: (a) The micro-channel heat pipe can reduce the amount of TEG and save the cost significantly than the conventional PV-TE system; (b) Micro-channel heat pipe has a higher heat transfer performance than the common heat pipe, so the new system has a high heat transfer performance; (c) Flat plate structure of the micro-channel heat pipe can be lamination with the PV and TE well and reduce the contact thermal resistance significantly between them; (d) The low temperature gradient can keep a high electrical output of PV and TE; (e) Comparison with the conventional PV system, the PV-TE has the higher output performance and economic value.

Acknowledgment

The study was sponsored by the National Science Foundation of China (Grant Nos. 51408578, 51611130195), Anhui Provincial Natural Science Foundation (1508085QE96), Dong Guan Innovative Research Team Program (No. 2014607101008).

References

[1] D.N. Kossyvakis, G.D. Voutsinas and E.V. Hristoforou, Experimental analysis and performance evaluation of a tandem photovoltaic–thermoelectric hybrid system, *Energy Convers Manage* **117**, 2016, 490–500.

[2] V. Avrutin, N. Izyumskaya and H. Morko, Semiconductor solar cells: recent progress in terrestrial applications, *Superlatt Microstruct* **49** (4), 2011, 337–364.

[3] Guiqiang Li, Gang Pei, Jie Ji, Ming Yang, Su Yuehong and Xu Ning, Numerical and experimental study on a PV/T system with static miniature solar concentrator, *Sol Energy* **120**, 2015, 565–574.

[4] Guiqiang Li, Gang Pei, Ming Yang, Jie Ji and Su Yuehong, Optical evaluation of a novel static incorporated compound parabolic concentrator with photovoltaic/thermal system and preliminary experiment, *Energy Convers Manage* **85**, 2014, 204–211.

[5] Guiqiang Li, Gang Pei, Jie Ji and Su Yuehong, Outdoor overall performance of a novel air-gap-lens-walled compound parabolic concentrator (ALCPC) incorporated with photovoltaic/thermal system, *Appl Energy* **144**, 2015, 214–223.

[6] Wei He, Gan Zhang, Xingxing Zhang, Jie Ji, Guiqiang Li and Xudong Zhao, Recent development and application of thermoelectric generator and cooler, *Appl Energy* **143**, 2015, 1–25.

[7] Y. Deng, W. Zhu, Y. Wang and Y.M. Shi, Enhanced performance of solar-driven photovoltaic–thermoelectric hybrid system in an integrated design, *Sol Energy* **88**, 2013, 182–191.

[8] J. Zhang, Y. Huan and L. Yuang, Performance estimation of photovoltaic thermoelectric hybrid systems, *Energy* **78**, 2014, 895–903.

[9] Y. Wu, S. Wu and L. Xiao, Performance analysis of photovoltaic–thermoelectric hybrid system with and without glass cover, *Energy Convers Manage* **93**, 2015, 151–159.

[10] J. Lin, T. Liao and B. Lin, Performance analysis and load matching of a photovoltaic–thermoelectric hybrid system, *Energy Convers Manage* **105**, 2015, 891–899.

[11] D. Kraemer, L. Hu, A. Muto, X. Chen, G. Chen and M. Chiesa, Photovoltaic–thermoelectric hybrid systems: a general optimization methodology, *Appl Phys Lett* **92** (24), 2008, 243503.

[12] M. Mizoshiri, M. Mikami and K. Ozaki, Thermal–photovoltaic hybrid solar generator using thin-film thermoelectric modules, *Jpn J Appl Phys* **51**, 2012, 06FL07.

[13] J.P. Fleurial, Thermoelectric power generation materials: technology and application opportunities, *J Miner, Met Mater Soc* **61** (4), 2009, 79–85.

[14] W. Van Sark, Feasibility of photovoltaic–thermoelectric hybrid modules, *Appl Energy* **88** (8), 2011, 2785–2790.

[15] H. Hashim, J.J. Bomphrey and G. Min, Model for geometry optimisation of thermoelectric devices in a hybrid PV-TE system, *Renew Energy* **87** (1), 2016, 458–463.

[16] R. Bjørk and K.K. Nielsen, The performance of a combined solar photovoltaic (PV) and thermoelectric generator (TEG) system, *Sol Energy* **120**, 2015, 187–194.

[17] W.Q. Lin, T.M. Shih, J.C. Zheng, Y.F. Zhang and J.C. Chen, Coupling of temperatures and power outputs in hybrid photovoltaic and thermoelectric modules, *Int J Heat Mass Transf* **74**, 2014, 121–127.

[18] Y. Da, Y.M. Xuan and Q. Li, From light trapping to solar energy utilization: a novel photovoltaic–thermoelectric hybrid system to fully utilize solar spectrum, *Energy* **95**, 2016, 200–210.

[19] T.F. Cui, Y.M. Xuan and Q. Li, Design of a novel concentrating photovoltaic–thermoelectric system incorporated with phase change materials, *Energy Convers Manage* **112**, 2016, 49–60.

[20] N. Wang, L. Han, H.C. He, N.H. Park and K. Koumoto, A novel high-performance photovoltaic–thermoelectric hybrid device, *Energy Environ Sci* **4**, 2011, 3676–3679.

[21] Adham Makki, Siddig Omer, Su Yuehong and Hisham Sabir, Numerical investigation of heat pipe-based photovoltaic–thermoelectric generator (HP-PV/TEG) hybrid system, *Energy Convers Manage* **112** (15), 2016, 274–287.

[22] Y.C. Deng, Y.H. Zhao, W. Wang, Z.H. Quan, L.C. Wang and D. Yu, Experimental investigation of performance for the novel flat plate solar collector with micro-channel heat pipe array (MHPA-FPC), *Appl Therm*

Eng **54** (2), 2013, 440–449.

[23] Guiqiang Li, Gan Zhang, Wei He, Jie Ji, Song Lv, Xiao Chen, et al., Performance analysis on a solar concentrating thermoelectric generator using the micro-channel heat pipe array, *Energy Convers Manage* **112**, 2016, 191–198.

[24] Li Guiqiang, Su Pei Gang, Ji Jie Yuehong and Saffa B. Riffat, Experiment and simulation study on the flux distribution of lens-walled compound parabolic concentrator compared with mirror compound parabolic concentrator, *Energy* **58**, 2013, 398–403.

[25] Wei He, Gan Zhang, Guiqiang Li and Jie Ji, Analysis and discussion on the impact of non-uniform input heat flux on thermoelectric generator array, *Energy Convers Manage* **98**, 2015, 268–274.

[26] G. Min, ZT measurements under large temperature differences, *J Electron Mater* **39** (9), 2010, 1782–1785.

[27] G. Min, Thermoelectric module design under a given thermal input: theory and example, *J Electron Mater* **42** (7), 2013, 2239–2242.

[28] H. Hashim, J.J. Bomphrey and G. Min, Model for geometry optimisation of thermoelectric devices in a hybrid PV/TE system, *Renew Energy* **87**, 2016, 458–463.

[29] T.L. Bergman, F.P. Incropera and A.S. Lavine, Fundamentals of heat and mass transfer, 2011, John Wiley & Sons.

[30] Li Guiqiang, Ji Jie, Zhang Gan, He Wei, Chen Xiao, Chen Hongbing. Performance analysis on a novel micro-channel heat pipe evacuated tube solar collector-incorporated thermoelectric generation. http://dx.doi.org/10.1002/er.3589.

[31] Adham Makki, Siddig Omer, Yuehong Su and Hisham Sabir, Numerical investigation of heat pipe-based photovoltaic–thermoelectric generator (HP-PV/TEG) hybrid system, *Energy Convers Manage* **112**, 2016, 274–287.

Highlights

- A novel PV-TE system was presented.
- Mathematical model of the system was built.
- Performance under different ambient conditions was analyzed.
- New PV-TE and the conventional PV were compared.
- Preliminary economic analysis was demonstrated.

Queries and Answers

Query: Your article is registered as a regular item and is being processed for inclusion in a regular issue of the journal. If this is NOT correct and your article belongs to a Special Issue/Collection please contact j.mani@elsevier.com immediately prior to returning your corrections.
Answer: yes.

Query: The author names have been tagged as given names and surnames (surnames are highlighted in teal color). Please confirm if they have been identified correctly.
Answer: yes

Query: Please note that Fig. 11 was not cited in the text. Please check that the citations suggested by the copyeditor are in the appropriate place, and correct if necessary.
Answer: Yes

Query: One or more sponsor names may have been edited to a standard format that enables better searching and identification of your article. Please check and correct if necessary.
Answer: yes

Query: The country names of the Grant Sponsors are provided below. Please check and correct if necessary. ‘National Science Foundation of China’ - ‘China’, ‘Anhui Provincial Natural Science Foundation’ - ‘China’.
Answer: yes